Synthesis and Surface Modification of Highly Fluorescent Gold Nanoclusters and Their Exploitation for Cellular Labeling

Cheng-An J. Lin[a, e], Chih-Hsien Lee[a, e], Jiun-Tai Hsieh[a, e], Wan-Chun Yu[a, e], Hong-Zhi Yang[a, e], Jimmy K. Li[f], Ralph Sperling[b], Hsueh-Hsiao Wang[c], Hung-I Yeh[c], Wolfgang J. Parak[b], Walter H. Chang[a, e]*

[a] Department of Biomedical Engineering, Chung Yuan Christian University, Chung-Li , Taiwan (R.O.C.); [b]Fachbereich Physik, Philipps Universität Marburg, Renthof 7, 35037 Marburg (Germany); [c]Cardiac Medicine, Mackay Memorial Hospital, Taipei, Taiwan (R.O.C.); [d]Department of Physics, Chung Yuan Christian University, Chung-Li , Taiwan (R.O.C.); [e] Center for Nano Bioengineering, Chung Yuan Christian University, Chung-Li , Taiwan (R.O.C.); [f] Department of Material Science, National University of Tainan, Tainan 70005 Taiwan (R.O.C.)

*Correspondence: whchang@cycu.edu.tw; phone 886 3 2654503; fax 886 3 2654581

ABSTRACT

We introduce a general approach to make colorful fluorescent gold nanoclusters which are protected by dihydrolipoic acid, mercaptoundecanoic acid and polyethylenimine. The fluorescent gold nanoclusters can perform a variety of bioconjugation processes such as PEGylation, biotinylation as well as forming complex nanobioconjugates with streptavidins. The brightening effects under proper surface modification are also reported. The clusters have a decent quantum yield, high colloidal stability, and can be readily conjugated with biological molecules. Nonspecific uptake by human aortic endothelial cells is demonstrated.

Keywords: fluorescent gold nanoclusters, bioconjugation, near infrared, cell labeling, PEGylation, biotinylation, lipoic acid

1. INTRODUCTION

Gold nanoclusters with size smaller than 2 nm have been gained great attention in the last decade for their unique role in bridging the link between atomic and nanoparticle behavior[1]. Researches have focused on their quantum physical properties including photoluminescence[2-9], optical chirality[10-13], ferromagnetism[14], and its practical applications including single molecule optoelectronics[15, 16], sensing[17] and bioassay[18, 19]. Similar to semiconductor quantum dots containing strong quantum-size confinement [20], gold nanoparticles give the size-dependent plasmon absorption band when their conduction electrons in both the ground and excited states are confined to dimensions smaller than the electron mean free path (ca. 20 nm)[21]. But the plasmon absorption of gold nanoparticles less than 2 nm disappears completely which can not be fitted by Mie's theory[22-24]. Interestingly, gold nanoclusters have a second critical size regime comparable to the Fermi wavelength of the electron (ca. 0.7 nm), resulting in molecule-like properties including size-dependent fluorescence[1, 17] and discrete electronic states[25-28]. Although the most well-studied semiconductor quantum dots (QDs) have become a new class of fluorescent labels[29, 30] due to unique optical properties as well as offering potential invaluable benefits such as cancer targeting[31] and biomedical imaging[32, 33], the containing heavy metals that are toxic makes them unsuitable for in vivo clinical application and may pose risks to human health as well as the environment under certain condition[34]. In contrast to QDs, which are larger in dimensions (3 to 100 nm), noble metal NCs are highly attractive for bioimaging and biolabeling applications because of their nontoxicity and ultrafine size. Color-tunable emission of fluorescent metallic nanoclusters has been developed recently[1, 17, 35, 36] but there is no general route to fabricate good quality of nanoclusters emitters. The emission wavelength correlates with not only its size but also its protected molecules. Current metallic nanoclusters using the template-based synthesis (i.e. dendrimer (PAMAM)[1], oligonucleotide (DNA)[36], proteins(BSA)[37], polyelectrolyte, polymer(PMAA)[38]) , monolayer-protected nanoclusters (MPCs) synthesis (i.e. dihydrogen lipoic acid (DHLA)[39], and mercaptoundecanoic acid(MUA)[40]) are illustrated in Figure 1.[41] Here we presented a novel synthetic method for multicolor gold nanoclusters with biocompatible surface as well as its cellular labeling application.

Colloidal Quantum Dots for Biomedical Applications V, edited by Marek Osinski, Wolfgang J. Parak, Thomas M. Jovin, Kenji Yamamoto, Proc. of SPIE Vol. 7575, 757506

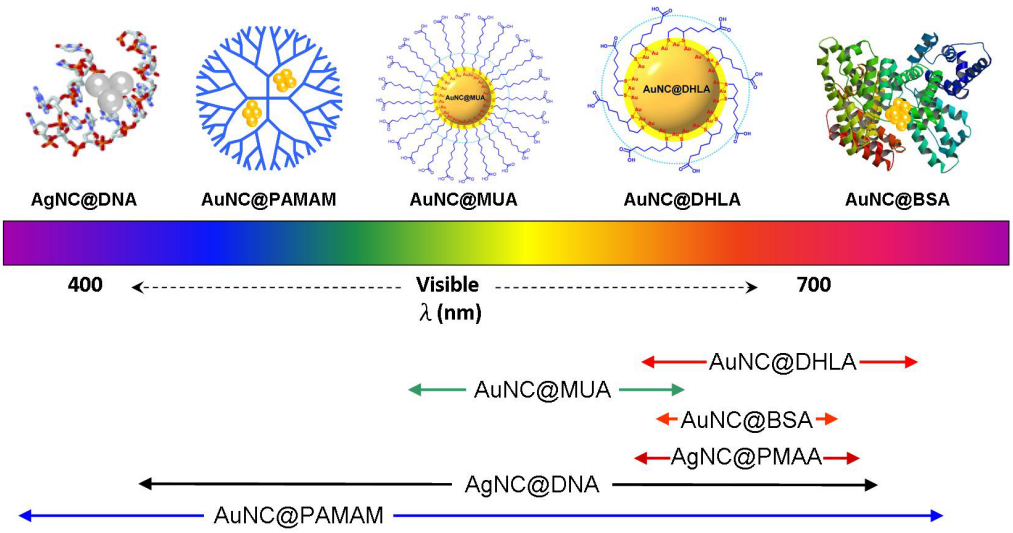

Figure 1. Representative fluorescent noble-metal nanoclusters scaled as a function of their emission wavelength superimposed over the spectrum. Fluorescent metallic nanoclusters can be protected by ether template (AgNC@DNA[36], AuNC@BSA[37], AuNC@PAMAM[1], AgNC@PMAA[38]) or monolayer ligands (AuNC@DHLA[39], AuNC@MUA[17]).

2. MATERIALS AND METHODS

2.1 Chemicals

Didodecyldimethylammonium bromide (DDAB, >98% purity; Fluka), decanoic acid (>98% purity, Aldrich), tetrabutylammonium borohydride (TBAB, >97% purity, Fluka), gold (III) chloride (AuCl3, 99% purity, Strem Chemicals), gold (III) chloride trihydrate ($HAuCl_4.3H_2O$), (±)-α-lipoic acid (≥99% purity, Sigma) ,and toluene (Sigma) were used.

2.2 Synthesis of Red-Near Infrared Emitted Gold Nanoclusters

The synthesis of 6 nm gold nanoparticles was modified from Peng's protocol of a single-phase reaction[42]. The Au precursor solution then etched the initial gold nanoparticles into small clusters. In brief, DDAB or decanoic acid was prepared in toluene as stock solution of 100 mM concentration. The Au precursor solution (25 mM) was prepared by dissolving an gold(III) chloride ($AuCl_3$ or $HAuCl_4$) in the DDAB solution. Typically, 1 ml of TBAB solution (100 mM in DDAB stock solution) and 0.625 ml decanoic acid stock solution was firstly mixed vigorously, followed by 0.8 ml gold precursor solution addition to form a dark-red solution of Au nanoparticles instantaneously. Upon addition of several drops of Au precursor solution under vigorous stirring, the solution color turned from dark-red color to a yellowish transparent solution. The vanishing of surface plasmon absorption around 520~530 nm attribute to the etching of Au nanoparticles to smaller Au nanoclusters (AuNC@DDAB). The as-prepared Au nanoclusters (AuNC@DDAB) were not fluorescent and became red fluorescent upon ligand exchange by dithiol molecules. The 0.0322 g of TBAB powder was dissolved in 2.5 ml of DDAB solution until no solid powders remained, followed by injecting into 0.052 g of lipoic acid (LA) powder until no more bubbles were generated. All lipoic acid was reduced into dihydrogenlipoic acid (DHLA) in this step. Another 0.052g of lipoic acid powder was again added in excess into the reduced lipoic acid mixture in order to eliminate residual activity of the TBAB reducing agent. In this way the final molar ratio of LA/TBAB which was 4/1. 2.5 ml of etched Au nanoclusters was added into the equivalent DHLA solution in toluene under vigorous stirring. The solution formed a yellow-brown agglomeration due to polar surface forming on nanoclusters. The nanoclusters agglomerates gradually became red-fluorescent upon UV exposure, which could be observed by naked eye. After removing the supernatant, the brown precipitate of DHLA-capped Au nanoclusters (AuNC@DHLA) was washed two times by toluene and finally re-dissolved in methanol. All solvents were then evaporated under reduced pressure by a rotavapor system (Laborota 4000, Heidolph). Adding 5 ml of 0.1 M NaOH the nanoclusters was soluble in the water phase due to the deprotonation of the COOH groups of the dried AuNC@DHLA. Filtration through a syringe membrane

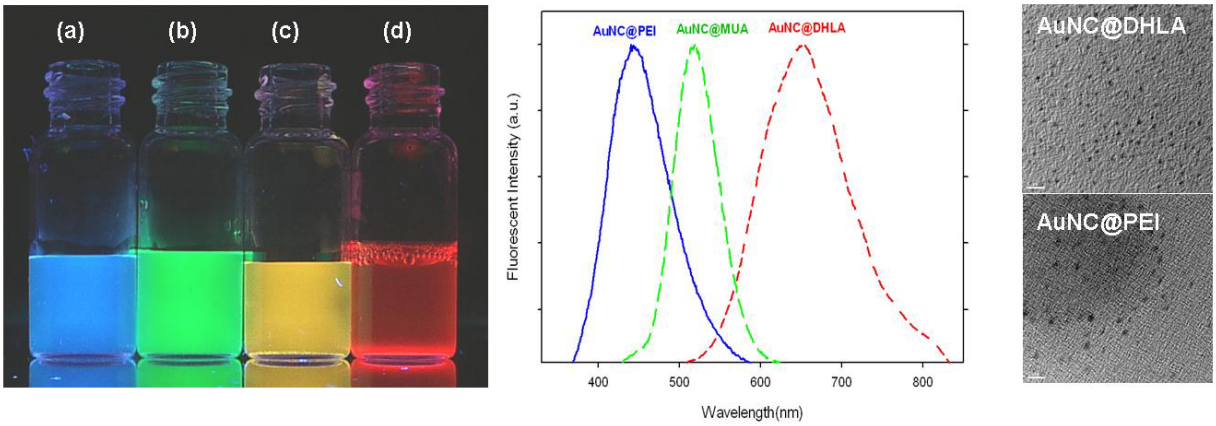

Figure 2. Fluorescent gold nanoclusters with different emissions. *Left:* (a) AuNC@PEI; (b,c)AuNC@MUA; (d)AuNC@DHLA; *Middle:* Emission spectrum of fluorescent gold nanoclusters; *Right:* TEM images of AuNC@DHLA and AuNC@PEI. Scale bar: 5 nm.

filter (Roth # P818.1, 0.22 μm pore size) helped to remove any remaining particle aggregated from solution. The Aunanoclusters were then purified by passing through the membrane of a 100 kDa MWCO centrifuge filter (Millipore) and concentrated by a 30 kDa MWCO centrifuge filter. The buffer could be changed via several runs of dilution and concentration cycles by the centrifuge filter if necessary. All the fluorescent Au nanoclusters were then precipitated (two times) with centrifugation at higher speed (usually 110,000 r.p.m. for 4 hours), which allowed for removing possible residues of free surfactant by discarding the supernatant.

2.3 Synthesis of Green-emitted Gold Nanoclusters

The green-emitted Au nanoclusters were modified from Huang et al.[17]. Firstly, 24 μL tetrakis(hydroxymethyl) phosphonium chloride (THPC) solution added to 50 mL of 20 mM NaOH for 5 mins and then it was mixed with gold(III) chloride solution (1.2 mM, 250 μL) for 15 mins, forming the Au nanoparticles (AuNP@THPC) for further ligand exchange with 11-mercaptoundecanoic acid (MUA). The 500 uL of 20 mM MUA in 10 mM tetraborate buffer (pH 9.2) was added into the as-prepared AuNP@THPC (500 uL). The mixtures were then left for ligand exchange for 72 h in the dark at room temperature to form the AuNC@MUA. Changing the THPC-to-$HAuCl_4$ concentration ratios could tune the emissive wavelength from green (1.0) to yellow (2.0) without losing quantum yield (Figure 2). The fluorescent AuNC@MUA was purified by conducting centrifugal filtration (13,500 g) for 40 min through a filter having a cutoff of 10 kDa. Most of the MUA and precursors in the solution were removed. The fluorescence of the removed solution showed a very weak luminescence when excited at 375 nm, indicating the luminescence signal was truly from 11-MUA–Au NDs.

2.4 Synthesis of Blue-emitted Gold Nanoclusters

Typically, $HAuCl_4.H_2O$ or polyethylenimine (PEI, Mn= 25,000 g/mol) was freshly dissolved in d.d.H_2O. Equivalent amount of gold chloride solution and PEI were mixed together vigorously and the solution turned to red immediately. All the mixture solution was kept in dark for three days. The blue luminescent nanoclusters were formed and purified by removing the larger agglomerates via passing through a filter having a cutoff of 10 kDa. All the samples were concentrated by freeze-drying. (Figure 2)

2.5 Size Characterization

The size distribution of the fluorescent Au nanoclusters was characterized by several techniques: transmission electron microscopy (TEM), size exclusion chromatography (SEC), atomic force microscopy (AFM), and gel electrophoresis[43]. *TEM* was used for visualizing the shape as well as measuring the diameter of the inorganic Au particles. TEM images were with a JEOL electron microscope operated at an accelerating voltage of 200 kV. The as-prepared Au nanoclusters were directed dried on carbon supported copper grids (#01822-F ultra-thin carbon type–A from Ted Pella Inc.). In case of DHLA-capped Au nanoclusters the particles were first dissolved in methanol prior to

depositing them on the TEM grids. The average size distribution of particles was determined from the TEM images by using the image analysis software "ImageJ" which is available at the NIH website http://rsb.info.nih.gov/ij/. The 100 particles per image were selected for statistic analysis. The hydrodynamic diameter of the Au nanoclusters was determined with *size exclusion chromatography using a Sephacryl S-200 column*. Methoxy-polyethylene glycol (mPEG, Rapp Polymere) of different molecular weight was used as standards[44] to correlate the elution time with the hydrodynamic diameter. The hydrodynamic diameter includes the size of the inorganic core plus two times the thickness of the organic shell around it. The *gel electrophoresis* was used as additional method to investigate the hydrodynamic diameter. The lager the nanoparticles are, the slower their mobility is. Two types of hydrophobic nanoparticles were then transferred into aqueous phase by capping them with reduced lipoic acid (DHLA): the original Au nanoparticles before etching (AuNP@DHLA) and the Au nanoclusters after etching (AuNC@DHLA). As reference 10-nm and 5-nm colloidal Au nanoparticles (BBInternational) coated with bis(p-sulfonatophenyl)phenylphosphine (Strem) were run simultaneously on the same gel. The gel electrophoresis was performed with 2% agarose gels for 20 mins (7.5 V/cm, Sub-Cell GT electrophoresis cells, Bio-Rad). The gel images were taken with a Pentax Optio mx4 camera, whereby the fluorescence images were recorded with UV excitation (365 nm) and the UV background was later removed using Photoimpact-v.12.

2.6 Photostability Test

Photostability was measured by recording the intensity change of fluorescent Au nanoclusters upon continuous photoexcitation. The 20 µl of fluorescent Au nanoclusters dissolved in sodium borate buffer (pH 9) loaded into a quartz cuvette with small capacity were entirely exposed to blue-light (480 nm) excitation from the Xenon lamp of the used fluorometer. Fluorescence intensity at 680 nm was recorded over time. Here we compared the photostability of fluorescent Au nanoclusters with two organic fluorophores as well as with one quantum dot sample. Rhodamine 6G and fluorescein (Sigma) were dissolved in sodium borate buffer (SBB, pH 9). Hydrophobic quantum dots (QD520, Evident Technology) were coated with an amphiphilic polymer (75% dodecylamine-modified poly(isobutyl-maleic anhydride)) and dissolved in SBB solution[45]. All samples were first adjusted to equal optical density (0.08) at 480 nm before recording their photostability. Fluorescence spectra were recorded every second by a fluorescence spectrometer (Fluorolog-3, Jobin Yvon) equipped high-power Xenon lamp and the intensities were plotted versus time. The excitation bandwidth was set to 20 nm and samples were loaded into small cuvettes (20 µl capacity).

2.7 Bioconjugation

For linkage with PEG, purified fluorescent AuNC@DHLA (15 µM in SBB), X-PEG-amine (3 mM methoxy-PEG5k-NH_2 or biotin-PEG5k-NH_2 in ddH2O), and EDC (aliquoted in seven fractions out of which each one had half of the EDC concentration 8 mM) was mixed equivalently (10 µL of each). After two hours of reaction, the fluorescent Au nanoclusters were run through gel electrophoresis with a 2% agarose gel (20 min, 7.5V/cm, Sub-Cell GT electrophoresis cells, Bio-Rad). Images of the gels were taken with a Pentax Optio mx4 camera. Fluorescence images were collected under 365 excitation and UV background removal using Photoimpact-v.12 software. In a next step proteins can also be directly attached to the surface of fluorescent Au nanoclusters using EDC. First, streptavidin (Sigma; A9275) as example of a protein was suspended in double distilled water to a final concentration of 1 mg/ml. The 128 mM EDC solution (Sigma) in double distilled water was prepared and aliquoted in seven fractions, out of which fraction contained one fourth of the EDC concentration compared to the previous fraction. EDC (10 µl) was added into mixture containing fluorescent AuNC@DHLA (10 µl, 15µM in SBB-pH7.4) and avidin (10 µl). After two hours reaction the fluorescent AuNC@DHLA were run through gel electrophoresis with 2% agarose gels (20 min, 7.5V/cm, Sub-Cell GT electrophoresis cells, Bio-Rad). For scale-up, 1 ml of EDC in double distilled H_2O was added to a mixture of fluorescence AuNC@DHLA (15 µM, 1 ml) and avidin (1 mg/ml, 1 ml) and the mixture was reacted for two hours.The unreacted sample was removed by passing a 100 kDa MWCO Amicon centrifuge filter (Millipore). Non-reacted AuNC@DHLA as well as avidin passes through the membrane, whereas the AuNC@DHLA with attached avidin could not pass the membrane. After several runs of washing, the fluorescent AuNC@DHLA-avidin conjugates were concentrated with the centrifuge filters to a volume of 200 ul in sodium borate buffer (SBB, pH 9). For antibody conjugation, 6 mg cysteamine was added into 1 mL anti-mouse IgG solution for 90 minutes in 37°C water bath, resulting in cleaved IgG antibody (i.e. half antibody). Free cysteamines were removed by dialysis with 10 kDa MWCO membrane against sodium phosphate buffer (150 mM NaCl, 10 mM EDTA). Concentrated half IgG and AuNC@DHLA were incubated overnight, resulting in spontaneously linkage through thiol-gold binding. The bioconjugates can be collected by a 100 kDa MWCO centrifuge filter and discarding the passing solution of free half IgG as well as AuNC@DHLA.

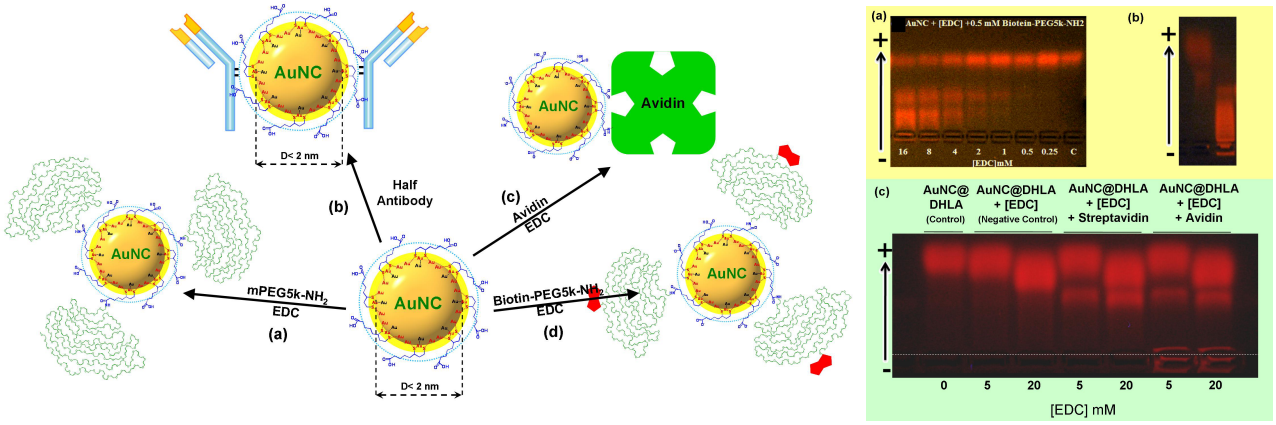

Figure 3. *Left*: Illustration of the conjugation of fluorescent Au nanoclusters (AuNC@DHLA) with (a) mPEG-amine, (b) antibody, (c) avidin and (d) biotin-PEG-amine; *Right*: (a) PEGylation of fluorescent Au nanoclusters with series EDC concentration; (b) Antibody + half antibody; (c) EDC-activated gold nanoclusters + streptavidin or avidin. The shifted band on gel electrophoresis showed the bioconjugates complex from Au nanoclusters (fastest band).

2.8 Cell labeling

For living cell labeling, human aortic endothelial cells (HAEC) was seeded onto 2% gelatin-coated glass coverslips and maintained in medium 200 with low serum growth supplement (all from Cascade Biologics) in an incubator under a humidified 95% air and 5% CO_2 37 °C atmosphere. HAEC cells passage 8 were used for incubation with fluorescent AuNC@DHLA. Fluorescent Au nanoclusters were added to the culture medium (containing serum and antibiotics) and condition medium (serum and antibiotics free medium). After 5 hours of incubation the uptake of AuNC@DHLA was tested. For this purpose cells were fixed with 2% paraformaldehyde, washed with PBS, followed by bisbenzimide staining (18.7 µmol/l) of the nuclei for 15 min, washed with PBS, and finally immersed in 60% glycerol (v/v). Images were then recorded with an optical microscope (DM IRBE; Leica, DC 300F CCD camera, Leica). Fluorescence images were recorded with 340–380 / 425 nm and 515–560 / 590 nm excitation / emission for the visualization of bisbenzimide and fluorescent AuNC@DHLA, respectively.

3. RESULTS AND DISCUSSION

We introduce a general approach to make colorful nanoclusters in water phase. In the synthesis of Au nanocluters with red emission, Au nanoparticles prepared from a one-phase reaction either with or without purification by methanol precipitation are etched into small nanoclusters by the Au precursor solution. The etched Au nanoclusters lose their surface plasmon properties and lead to a yellowish or even colorless transparent solution, whereas the original larger Au nanoparticles possess strong surface plasmon absorption around 520~530 nm. The etching process can induce by various Au precursors such as $AuCl_3$, $HAuCl_4$, $AuBr_3$, and $HAuBr_4$. Etching (observed by vanishing of the surface plasmon absorption) could be also observed in the case when the particles were not precipitated and purified with methanol before adding the gold precursor solution. However, in this case the plasmon absorption increased in the beginning upon Au precursor addition, likely due to the residue of active reducing agents still in solution (i.e. TBAB), which resulted in growing of the nanoparticles. The plasmon peak then started to decrease upon further addition of new Au precursor solution via exhaustion of the reducing agents (which reduce gold precursors to Au nanoparticles) and eventually vanished. Therefore, when the Au particles were not purified prior the addition of Au precursor, the more Au precursor needed to be added for the etching of the nanoparticles until a final transparent solution was obtained. The addition of TBAB-reduced lipoic acid can replace the surfactants on the etched Au nanoclusters via the formation of strong dithiol-Au bonds, whereby the acid head group points towards the solution. Freshly-reduced lipoic acid (DHLA) contains two free thiol groups per molecule which are reactive towards the surfaces of the gold nanoclusters, whereas the oxidized forms of lipoic acids did not show to react when added into solutions of etched Au nanocluster. Upon such ligand exchange with lipoic acid the Au nanoclusters become red-emitting fluorophores. By deprotonization under basic buffer, the etched Au nanoclusters become water-soluble and form a mono-dispersion stabilized by electrostatic repulsion. The

as-prepared Au nanoparticles (AuNP@DDAB) had a core diameter of 5.55±0.68 nm. The sequential addition of Au precursors into the Au nanoparticles resulted in disappearance of the plasmon absorption, which is due to the etching of the particles. TEM images recorded on the resulting Au nanoclusters (AuNC@DDAB) indicate a diameter of 3.1±0.3 nm. Performing ligand exchange using DHLA on the Au nanoclusters further reduced the Au nanoclusters size to 1.5±0.3 nm (AuNC@DHLA). The Au nanoclusters were also found to be crystalline. From size exclusion chromatography data, the Au nanoclusters elute at the same time like PEG molecules of 1 - 3 kDa molecular weights, with the peak coinciding with the 3 kDa PEG. This corresponds to hydrodynamic diameters ranging from 1.2 nm - 3.3 nm. For the synthesis of Au nanoclusters with blue emission, PEI in d.d.H_2O resulted in basic solution and can directly reduced the gold ions. The PEI-protected Au nanoparticles were formed immediately and then larger Au nanoclusters during prolong incubation. The unstable nanoparticle became agglomerate, precipitate and resulted in transparent solution which contains bright blue emission under UV lamp. The blue fluorophores attributes to the nanoclusters-PEI complex etching from Au nanoparticles. AuNC@PEI has an emission peak at 450 nm, which the fluorescence properties of both excitation and emission wavelength are similar to those of PAMAM-encapsulated Au8 clusters as reported by Dickson group[8]. TEM images (Figure 2) recorded on the resulting Au nanoclusters (AuNC@PEI) indicate a diameter of 2 nm, indicating the liberated clusters (Au8) are immediately protected by a multivalent and hyperbranched PEI ligand. The PEI ligand could also function to activate Au atoms and to subtract Au8 clusters from the nanocrystal surface. The formation of Au8 clusters probably results from the extraordinary stability of this "magic" cluster with closed electronic shell[46].

Photostability was measured by recording the fluorescent intensity change upon continuous photoexcitation. Most traditional organic fluorophores suffer from fast photobleaching upon optical excitation. Core/shell quantum dots have been demonstrated to possess high photostability. Three water-soluble fluorescent materials, CdSe/ZnS quantum dots (polymer-coated QD520), Rhodamine 6G and fluorescein, were selected for comparison under the same excitation wavelength. All samples were adjusted to the same optical density at 480 nm before recording the PL intensity. As shown in Figure 3, the organic fluorophore shows fast photobleaching, which is not present in the case of semiconductor quantum dots. The fluorescent Au nanoclusters exhibited a slower photobleaching rate than the organic fluorophores, though not as good as the semiconductor quantum dots. The half life of fluorescent Au nanoclusters in comparison to the organic dye is 32000s vs. 2500s respectively in the test condition. Semiconductor quantum dots (CdSe/ZnS) showed an excellent photostability and did not photobleach within the observation time. Fluorescent Au nanoclusters photobleached faster than quantum dots but still much slower than traditional organic fluorophores.

The pair of thiol groups of each dihydrolipoic acid (DHLA) molecule binds to the surface of Au nanoclusters, so that the carboxylic acids protrude into solution and thus provide water-solubility. The Au-core diameter of the fluorescent Au nanoclusters is around 1~2 nm. (Biological) molecules containing amine-groups can be covalently linked to the carboxylic groups around the fluorescent Au nanoclusters by EDC crosslinker chemistry. As shown in Figure 3, water-soluble fluorescent Au nanoclusters were reacted with a mixture of EDC and biotin-PEG5k-amine for two hours. After extraction from the gel and purification of the retarded bands, which correspond to Au nanoclusters with exactly one attached PEG5k-biotin molecule, these biotinylated Au nanoclusters could further react with streptavidin in SBB-buffer (pH 9). The streptavidin did not show significant non-specific binding to the unconjugated Au nanoclusters. Addition of streptavidin to biotinylated Au nanoclusters on the other hand lead to the appearance of an additional retarded band, which we attribute to successful conjugation of biotinylated fluorescence Au nanoclusters and streptavidin. Furthermore, ether streptavidin or avidin offers functional group, which can link covalently with Au nanoclusters. EDC-activated Au nanoclusters formed larger conjugates with nanoclusters which were found in the retarded shifted band on the gel (Figure 3).

Because the fluorescent metallic nanoclusters have decent quantum yield and photostability, they can be used as cell markers for long-term studies such as cell-cell interactions, cell differentiation, and tracking. Human aortic endothelial cells can uptake the un-modified red-emissive Au nanoclusters after around 5 hr incubation as shown in Figure 4. Fluorescent metallic nanoclusters is based on the discovery that nanoclusters can be internalized by cells, by either receptor-mediated[47] or nonspecific endocytosis [39]. Blue-emissive Au nanoclusters functionalized with site-specific leading peptide such as SV40 NLS can enter the cytoplasm of living HeLa cells, where the non-functionalized ones shows no intracellular signalings for 1.5 hr treatment[47]. But the exact pathway of incorporating metallic nanoclusters into cells under endocytosis requires further investigation.

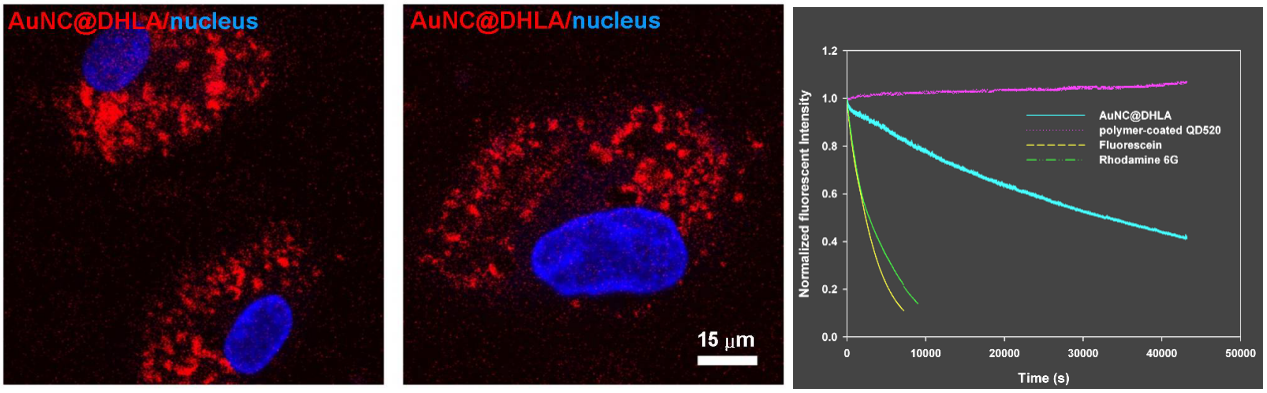

Figure 4. *Left:* Delivery of AuNC@DHLA in human aortic endothelial cells. The uptake of gold nanoclusters, shown in red fluorescence were examined using fluorescence microscopy. The blue fluorescence is nucleus counterstained with bisbenzimide. *Right:* Photostability over time of fluorescent Au nanoclusters (AuNC@DHLA) compared to semiconductor quantum dots (polymer-coated QD 520 from Invitrogen) and organic fluorophores (fluorescein, Rhodamine 6G)

4. CONCLUSION

In this report we describe the synthesis of multi-color fluorescent Au nanoclusters capped with various ligands such as DHLA, MUA and PEI. We demonstrated the related bio-conjugation chemistry for connecting to biological world. Fluorescent Au nanoclusters also showed good biocompatibility for living cells labeling. We believe that fluorescent Au nanoclusters have a great potential for applications to biomedical research to offer.

5. ACHNOWLEDGEMENTS

We gratefully acknowledge the supports of research grants from The National Science Council (NSC 98-2627-B-033-001, 98-2627-B-195-001), Mackay Memorial Hospital (MMH-E-98003), Department of Health of Taiwan (DOH 98-TD-N-111-001), and Specific Research Fields Project of Chung Yuan Christian University (CYCU-98-CR-BE). C.-A. J. Lin was supported by the NSC postdoctoral fellowship (NSC 098-2811-B-033-002).

REFERENCES

[1] Zheng, J., Zhang, C. W., and Dickson, R. M., "Highly fluorescent, water-soluble, size-tunable gold quantum dots," *Phys. Rev. Lett.,* 93(7), 077402, (2004).

[2] Bigioni, T. P., Whetten, R. L., and Dag, O., "Near-infrared luminescence from small gold nanocrystals," *J. Phys. Chem. B,* 104(30), 6983-6986, (2000).

[3] Huang, T. and Murray, R. W., "Visible luminescence of water-soluble monolayer- protected gold clusters," *J. Phys. Chem. B,* 105(50), 12498-12502, (2001).

[4] Peyser, L. A., Vinson, A. E., Bartko, A. P., and Dickson, R. M., "Photoactivated fluorescence from individual silver nanoclusters," *Science,* 291(5501), 103-106, (2001).

[5] Zheng, J. and Dickson, R. M., "Individual water-soluble dendrimer-encapsulated silver nanodot fluorescence," *J. Am. Chem. Soc.,* 124(47), 13982-13983, (2002).

[6] Link, S., Beeby, A., FitzGerald, S., El-Sayed, M. A., Schaaff, T. G., and Whetten, R. L., "Visible to infrared luminescence from a 28-atom gold cluster," *J. Phys. Chem. B,* 106(13), 3410-3415, (2002).

[7] Yang, Y. and Chen, S., "Surface Manipulation of the Electronic Energy of Subnanometer-Sized Gold Clusters: An Electrochemical and Spectroscopic Investigation," *Nano Lett.,* 3(1), 75-79, (2003).

[8] Zheng, J., Petty, J. T., and Dickson, R. M., "High quantum yield blue emission from water-soluble Au-8 nanodots," *J. Am. Chem. Soc.,* 125(26), 7780-7781, (2003).

[9] Negishi, Y., Takasugi, Y., Sato, S., Yao, H., Kimura, K., and Tsukuda, T., "Magic-numbered Au-n clusters protected by glutathione monolayers (n=18, 21, 25, 28, 32, 39): Isolation and spectroscopic characterization," *J. Am. Chem. Soc.,* 126(21), 6518-6519, (2004).

[10] Schaaff, T. G. and Whetten, R. L., "Giant gold-glutathione cluster compounds: Intense optical activity in metal-based transitions," *J. Phys. Chem. B,* 104(12), 2630-2641, (2000).
[11] Garzon, I. L., Reyes-Nava, J. A., Rodriguez-Hernandez, J. I., Sigal, I., Beltran, M. R., and Michaelian, K., "Chirality in bare and passivated gold nanoclusters," *Phys. Rev. B,* 66(7), 073403, (2002).
[12] Gautier, C. and Bürgi, T., "Chiral Inversion of Gold Nanoparticles," *J. Am. Chem. Soc.,* 130(22), 7077-7084, (2008).
[13] Roman-Velazquez, C. E., Noguez, C., and Garzon, I. L., "Circular Dichroism Simulated Spectra of Chiral Gold Nanoclusters: A Dipole Approximation," *J. Phys. Chem. B,* 107(44), 12035-12038, (2003).
[14] Crespo, P., Litran, R., Rojas, T. C., Multigner, M., de la Fuente, J. M., Sanchez-Lopez, J. C., Garcia, M. A., Hernando, A., Penades, S., and Fernandez, A., "Permanent magnetism, magnetic anisotropy, and hysteresis of thiol-capped gold nanoparticles," *Phys. Rev. Lett.,* 93(8), 087204, (2004).
[15] Lee, T. H., Gonzalez, J. I., Zheng, J., and Dickson, R. M., "Single-molecule optoelectronics," *Acc. Chem. Res.,* 38(7), 534-541, (2005).
[16] Vosch, T., Antoku, Y., Hsiang, J. C., Richards, C. I., Gonzalez, J. I., and Dickson, R. M., "Strongly emissive individual DNA-encapsulated Ag nanoclusters as single-molecule fluorophores," *Proc. Natl. Acad. Sci. U. S. A.,* 104(31), 12616-12621, (2007).
[17] Huang, C. C., Yang, Z., Lee, K. H., and Chang, H. T., "Synthesis of highly fluorescent gold nanoparticles for sensing Mercury(II)," *Angew. Chem., Int. Ed.,* 46(36), 6824-6828, (2007).
[18] Triulzi, R. C., Micic, M., Giordani, S., Serry, M., Chiou, W. A., and Leblanc, R. M., "Immunoasssay based on the antibody-conjugated PAMAM-dendrimer-gold quantum dot complex," *Chem. Commun.,* 48, 5068-5070, (2006).
[19] Huang, C. C., Chiang, C. K., Lin, Z. H., Lee, K. H., and Chang, H. T., "Bioconjugated gold nanodots and nanoparticles for protein assays based on photoluminescence quenching," *Anal. Chem.,* 80(5), 1497-1504, (2008).
[20] Alivisatos, A. P., "Semiconductor Clusters, Nanocrystals, and Quantum Dots," *Science,* 271(16), 933-937, (1996).
[21] Link, S. and El-Sayed, M. A., "Optical properties and ultrafast dynamics of metallic nanocrystals," *Annu. Rev. Phys. Chem. ,* 54, 331-66, (2003).
[22] Alvarez, M. M., Khoury, J. T., Schaaff, T. G., Shafigullin, M. N., Vezmar, I., and Whetten, R. L., "Optical absorption spectra of nanocrystal gold molecules," *J. Phys. Chem. B,* 101(19), 3706-3712, (1997).
[23] Schaaff, T. G., Shafigullin, M. N., Khoury, J. T., Vezmar, I., Whetten, R. L., Cullen, W. G., First, P. N., GutierrezWing, C., Ascensio, J., and JoseYacaman, M. J., "Isolation of smaller nanocrystal au molecules: Robust quantum effects in optical spectra," *J. Phys. Chem. B,* 101(40), 7885-7891, (1997).
[24] Hostetler, M. J., Wingate, J. E., Zhong, C. J., Harris, J. E., Vachet, R. W., Clark, M. R., Londono, J. D., Green, S. J., Stokes, J. J., Wignall, G. D., Glish, G. L., Porter, M. D., Evans, N. D., and Murray, R. W., "Alkanethiolate gold cluster molecules with core diameters from 1.5 to 5.2 nm: Core and monolayer properties as a function of core size," *Langmuir,* 14(1), 17-30, (1998).
[25] Apell, P., Monreal, R., and Lundqvist, S., "Photoluminescence of noble metals," *Phys. Scr.,* 38, 174-179, (1988).
[26] Chen, S., Ingram, R. S., Hostetler, M. J., Pietron, J. J., Murray, R. W., Schaaff, T. G., Khoury, J. T., Alvarez, M. M., and Whetten, R. L., "Gold nanoelectrodes of varied size: transition to molecule-like charging," *Science,* 280(5372), 2098-101, (1998).
[27] Lee, D., Donkers, R. L., Wang, G. L., Harper, A. S., and Murray, R. W., "Electrochemistry and optical absorbance and luminescence of molecule-like Au-38 nanoparticles," *J. Am. Chem. Soc.,* 126(19), 6193-6199, (2004).
[28] Lin, Z. Y., Kanters, R. P. F., and Mingos, D. M. P., "Closed-Shell Electronic Requirements for Condensed Clusters of the Group-11 Elements," *Inorg. Chem.,* 30(1), 91-95, (1991).
[29] Bruchez, M., Jr., Moronne, M., Gin, P., Weiss, S., and Alivisatos, A. P., "Semiconductor nanocrystals as fluorescent biological labels," *Small,* 281(5385), 2013-6, (1998).
[30] Chan, W. C. and Nie, S., "Quantum dot bioconjugates for ultrasensitive nonisotopic detection," *Small,* 281(5385), 2016-8, (1998).
[31] Smith, A. M., Dave, S., Nie, S. M., True, L., and Gao, X. H., "Multicolor quantum dots for molecular diagnostics of cancer," *Expert. Rev. Mol. Diagn.,* 6(2), 231-244, (2006).
[32] Alivisatos, A., Gu, W., and Larabell, C., "Quantum Dots as Cellular Probes," *Annu. Rev. Biomed. Eng.,* 7, 55-76, (2005).
[33] Michalet, X., Pinaud, F. F., Bentolila, L. A., Tsay, J. M., Doose, S., Li, J. J., Sundaresan, G., Wu, A. M., Gambhir, S. S., and Weiss, S., "Quantum dots for live cells, in vivo imaging, and diagnostics," *Science,* 307(5709), 538-44, (2005).
[34] Hardman, R., "A toxicologic review of quantum dots: toxicity depends on physicochemical and environmental factors," *Environ. Health Perspect.,* 114(2), 165-72, (2006).

[35] Diez, I., Pusa, M., Kulmala, S., Jiang, H., Walther, A., Goldmann, A. S., Muller, A. H. E., Ikkala, O., and Ras, R. H. A., "Color Tunability and Electrochemiluminescence of Silver Nanoclusters," *Angew. Chem., Int. Ed.,* 48(12), 2122-2125, (2009).
[36] Richards, C. I., Choi, S., Hsiang, J. C., Antoku, Y., Vosch, T., Bongiorno, A., Tzeng, Y. L., and Dickson, R. M., "Oligonucleotide-stabilized Ag nanocluster fluorophores," *J. Am. Chem. Soc.,* 130(15), 5038-5039, (2008).
[37] Xie, J. P., Zheng, Y. G., and Ying, J. Y., "Protein-Directed Synthesis of Highly Fluorescent Gold Nanoclusters," *J. Am. Chem. Soc.,* 131(3), 888-889, (2009).
[38] Shang, L. and Dong, S. J., "Facile preparation of water-soluble fluorescent silver nanoclusters using a polyelectrolyte template," *Chem. Commun.,* 9, 1088-1090, (2008).
[39] Lin, C.-A. J., Yang, T. Y., Lee, C. H., Huang, S. H., Sperling, R. A., Zanella, M., Li, J. K., Shen, J. L., Wang, H. H., Yeh, H. I., Parak, W. J., and Chang, W. H., "Synthesis, characterization, and bioconjugation of fluorescent gold nanoclusters toward biological labeling applications," *ACS Nano,* 3(2), 395-401, (2009).
[40] Huang, C. C., Liao, H. Y., Shiang, Y. C., Lin, Z. H., Yang, Z., and Chang, H. T., "Synthesis of wavelength-tunable luminescent gold and gold/silver nanodots," *J. Mater. Chem.,* 19(6), 755-759, (2009).
[41] Lin, C.-A. J., Lee, C.-H., Hsieh, J.-T., Wang, H.-H., Li, J. K., Shen, J.-L., Chan, W.-H., Yeh, H.-I., and Chang, W. H., "Synthesis of Fluorescent Metallic Nanoclusters toward Biomedical Application: Recent Progress and Present Challenges," *J. Med. Biol. Eng.*, 29(6), Accepted, (2009).
[42] Jana, N. R. and Peng, X. G., "Single-phase and gram-scale routes toward nearly monodisperse Au and other noble metal nanocrystals," *J. Am. Chem. Soc.,* 125(47), 14280-14281, (2003).
[43] Sperling, R. A., Liedl, T., Duhr, S., Kudera, S., Zanella, M., Lin, C.-A. J., Chang, W. H., Braun, D., and Parak, W. J., "Size determination of (bio-) conjugated water-soluble colloidal nanoparticles - a comparison of different techniques," *J. Phys. Chem. C,* 111(31), 11552-11559, (2007).
[44] Fee, C. J. and Alstine, J. M. V., "Prediction of the Viscosity Radius and the Size Exclusion Chromatography Behavior of PEGylated Proteins," *Bioconjugate Chem. ,* 15(6), 1304-1313, (2004).
[45] Lin, C.-A. J., Sperling, R. A., Li, J. K., Yang, T.-Y., Li, P.-Y., Zanella, M., Chang, W. H., and Parak, W. J., "Design of an amphiphilic polymer for nanoparticle coating and functionalization," *Small*, 4(3), 334-341, (2008).
[46] Duan, H. W. and Nie, S. M., "Etching colloidal gold nanocrystals with hyperbranched and multivalent polymers: A new route to fluorescent and water-soluble atomic clusters," *J. Am. Chem. Soc.,* 129(9), 2412-+, (2007).
[47] Lin, S. Y., Chen, N. T., Sum, S. P., Lo, L. W., and Yang, C. S., "Ligand exchanged photoluminescent gold quantum dots functionalized with leading peptides for nuclear targeting and intracellular imaging," *Chem. Commun.,* 39, 4762-4764, (2008).